

Energy Storage Using MnO₂ Supercapacitor Electrode

*M.M.El-Zaidia, A.H.Khafagy, S.Hassan and M.Z.Zaki

Physics Department, Faculty of science, Menoufia University, Shebeen El-Koom, Egypt

Corresponding Author: M.M.El-Zaidia

Abstract: The deposition of MnO₂ on stainless steel substrate was carried out using potentiostatic (PS) and galvanostatic (GS) deposition methods. Both deposited layers were found to be amorphous in nature. The SEM micrographs confirm this result. The I-V curves of the constructed supercapacitor show that the maximum and average stored electric power were 18 and 6.2 watt using PS deposition method. These values were independent on the voltage scan rate after 1000 cycle. The stored electric energy using PS was nearly one and half that stored using GS. The values of the stored energy were 91 and 73 joules using PS and GS, respectively. The maximum specific capacitance of the constructed supercapacitor was 389 and 327 Farad/gram for PS and GS respectively. The time constant of charge periods were 5×10^{-3} S, and 6.02×10^{-3} S, for both PS and GS films respectively, but the time constant for the discharging period for both of PS and GS films was the same, and has the value 1.02×10^{-3} seconds. The Nyquist plots of deposited MnO₂ films show features of porous electrodes. This means that their impedance are resistance at high frequency and capacitive at low frequency.

Keywords: Crystalline; Amorphous; electric power; energy storage; electric impedance.

Date of Submission: 14-08-2017

Date of acceptance: 13-09-2017

I. INTRODUCTION

Nowadays the energy crisis in the world increase, so world makes great attention to use of renewable energy sources and developing energy storages technologies. Energy storage systems are the way to manage the discontinuous nature of renewable sources¹. One of these systems is supercapacitor known also ultracapacitor or electrochemical capacitor which has high energy density, high power, short charge time, high safety, long cycle life and high efficiency²⁻⁶. There are two main categories of supercapacitor depending on active electrode material, double-layer capacitor where carbon is the base active material; pseudo-capacitor where conducting polymer or transition metal oxide is the active electrode^{3, 4, 6, 7}. Metal oxides are used because they have characterized properties like high conductivity and high specific capacitance^{1, 8} such as RuO₂^{9, 10}, IrO₂¹¹, MnO₂^{12, 13}, NiO, Co₂O₃, SnO₂, V₂O₅, or MoO_x¹. However most effective are Ruthenium and manganese oxides^{1, 14}. But RuO₂ is toxic and expensive⁴ unlike MnO₂ is abundant, eco-friendly and has promising electrochemical features¹⁵⁻¹⁷. Electrodeposition of manganese dioxide thin film can be obtained by anodic or cathodic technique¹⁸. Anodic electrochemical deposition method of MnO₂ is commonly used¹⁸. Manganese dioxide thin film is generally produced by anodic deposition onto metallic conductive substrate using acidified MnSO₄ solution. However, this method usually leads to the dissolution of the conductive substrate or build up an insulating oxide layer at the active oxide/substrate interface. Many techniques can be used for anodic deposition such as, potentiostatic, galvanostatic, potentiodynamic, and pulse deposition^{18, 19}. The aim of the present work is to study the electrochemically deposit thin films of MnO₂ on stainless steel substrate grade (304) as a current collector by anodic electrochemical deposition method using manganese acetate solution. This is to avoid the oxidation problems in acidic medium and applying both the potentiostatic and galvanostatic techniques, as a comparison study on the structural and electrochemical properties of deposited MnO₂ for supercapacitor application.

II. EXPERIMENTAL

2.1 Electrochemical deposition of MnO₂ films

Stainless-Steel (SS) foils commercially available (type 304) of thickness 0.175 mm were cut as samples of 1×2 cm² each to be used as working electrodes for the electrochemical deposition. The samples were first etched in Hydrochloric acid, 38% for 10 minutes, and then washed with distilled water and air dried. MnO₂ thin films were anodically electrodeposited from 0.25 M (CH₃COO)₂Mn.4H₂O solution by both potentiostatic (PS) and galvanostatic (GS) conditions at 1 volt and 1 mA/cm², respectively. The estimated mass loading of the deposited MnO₂ film was 300 μg/cm², which controlled by adjusting the total charge passed through the electrode during deposition time.

2.2 Structure and Electrochemical characterization of MnO₂/SS electrode:

The structural and morphological characteristics of prepared MnO₂ films were examined by X-ray diffraction (XRD) and scanning-electron microscope (SEM), respectively. The X-ray diffraction pattern of the film was recorded using automated and computerized Philips (model PW1051) supplied with monochromatic CuK α radiation source ($\lambda=1.541\text{\AA}$), while surface morphology of electrodeposited films was investigated using (Quanta 250 FEG) Scanning electron microscope.

All electrochemical deposition and measurements were performed by conventional three electrode system using SP-150 potentiostat /galvanostat device in an electrochemical cell with stainless steel substrate as a working electrode, Ag/AgCl (NaCl saturated) as a reference electrode, Pt wire as a counter electrode, and 0.5 M Na₂SO₄ solution as the characterization electrolyte. The deposited MnO₂ thin films were tested for supercapacitor application by studying the cyclic voltammetry, charge-discharge, and electrochemical impedance spectroscopy (EIS) measurements. Cyclic voltammetry (CV) tests were conducted in a potential range of 0-1 V at scan rates of 10-100 mV/s. Galvanostatic charge/ discharge cycling was conducted at current density of 1-10 mA/cm² between 0 and 1 volt. EIS data were collected at alternating current root mean square voltage amplitude 10 mV in a frequency range of 100 kHz-10MHz.

III. RESULTS AND DISCUSSION

3.1. Structure studies

X-ray studies

Fig(1) shows, the appearance of x-ray sharp peaks, reflecting the crystalline structure of the bare stainless steel (SS) substrate. After the potentiostatic deposition of MnO₂ on stainless steel substrate, the x-ray diffraction pattern was recorded once again.

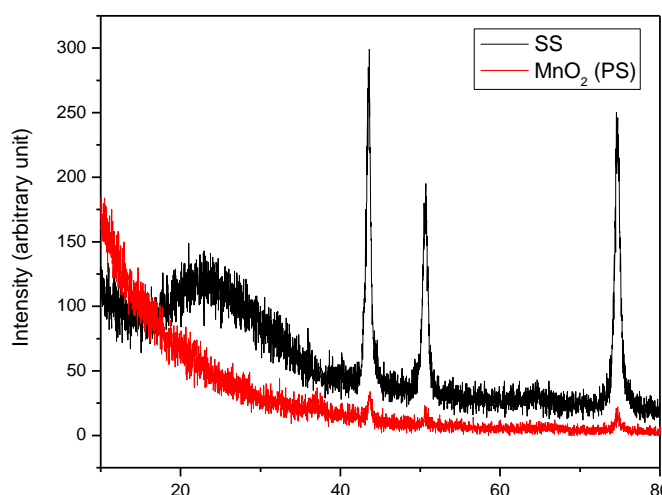


Fig.(1)XRD patterns of etched bare SS and potentiostatically deposited MnO₂/SS.

The obtained x-ray pattern confirms the amorphous nature of the deposited MnO₂ layer. The detected x-ray peaks roots which are superimposed on the pattern of MnO₂ at the same location of SS crystalline peaks may be due to higher order of x-ray reflections from SS substrate. This confirms the amorphous nature of the PS deposited film. However, the amorphous nature of the deposited metal oxide film is generally required for obtaining electrodes with large surface area for supercapacitor purposes, where the amorphous phase can give the chance for ions to penetrate the bulk active material^{2, 20}.

3.2.SEM Studies

Fig (2) (a-f) shows the SEM surface morphological micrographs for as-active bare SS(a), etched bare SS(b), potentiostatic deposition MnO₂ layer (c), and galvanostatic deposition MnO₂ layer (d) and potentiostatic deposited MnO₂ layer after 1000 cycles of charging and discharging (f). Referring to fig(2) it is clear that, the surface of both (a) and (b) micrographs has regular striped features. The features look like to be dim in image (a) and bright in image (b) as a result of different applied treatments.

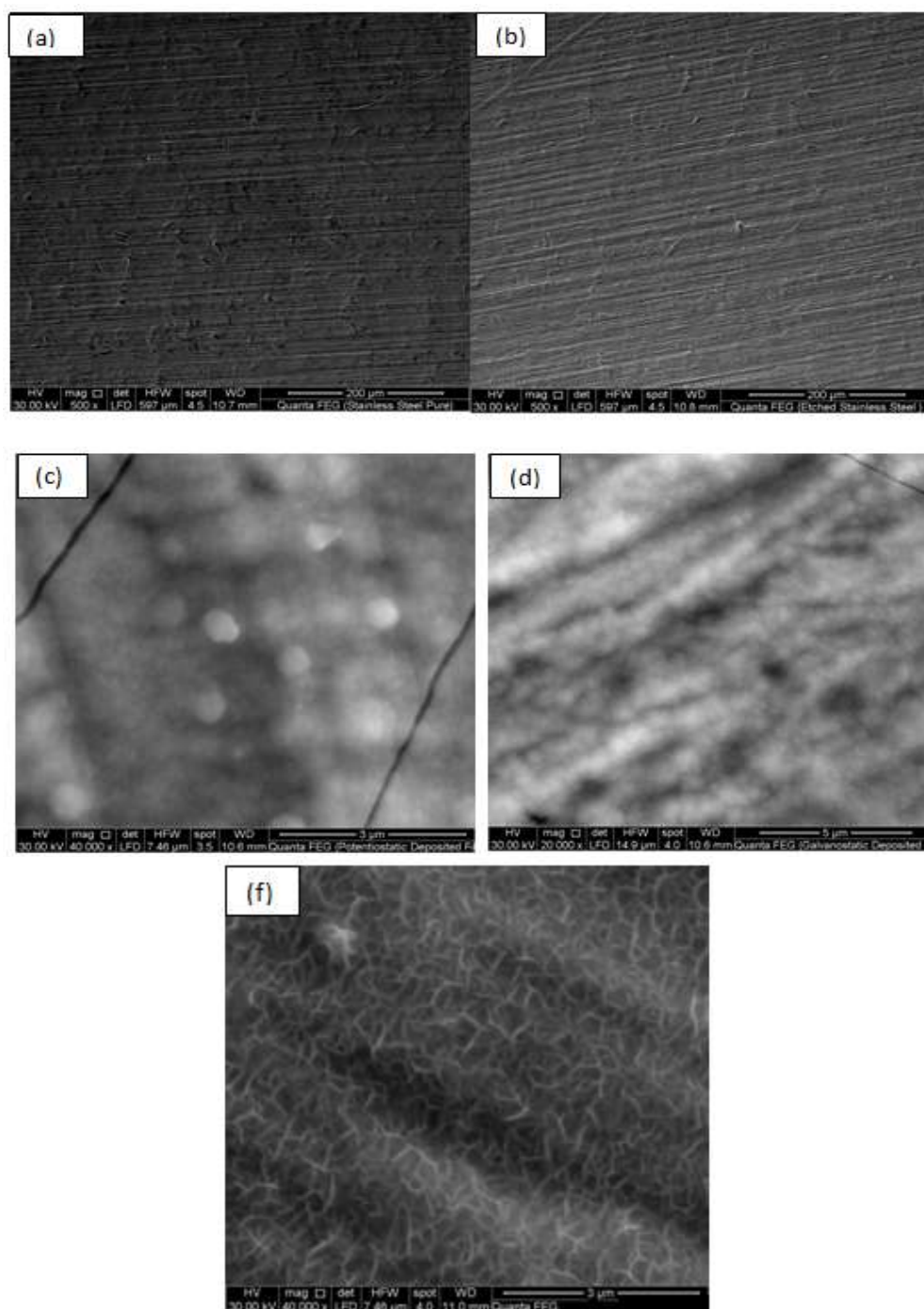


Fig.(2) SEM micrographs of (a) as received bare SS, (b) etched bare SS, (c) potentiostatically deposited MnO_2/SS , (d) galvanostatically deposited MnO_2/SS , (e) potentiostatically deposited MnO_2 after cyclic stability investigation.

Fig (2c) reveals irregular bright circles nearly of the same diameters (450nm). This may be represent the top view of some topological structures of MnO_2 layer as deposited potentiostatically. This micrograph reveals that the deposition of MnO_2 on SS was wavy heterogenous deposition, forming hills and valleys. The hills appear to be bright cylinders, while, the valleys appear to be dark grooves. Both of hills and valleys composed one unit domain with two different heights, but with well cross-linking. Fig(2f) shows the deposition of MnO_2 using PS after undergoing 1000 charging and discharging cycles. This multiprocess yields three dimensional growth (3DG) MnO_2 matrix.

As a result of this 3DG the deposition of MnO_2 matrix, becomes large enough to the possible effective polarization. These leads to the construction of supercapacitor of high capacity used as a great energy source.

3.3. Electrochemical capacitive behavior

3.3.1. Cyclic voltammetry

Fig(3a) shows the cyclic voltammetry(I-V) comparison curves for both PS and GS deposition methods for MnO₂ layers on etched SS electrodes measured in 0.5 M Na₂SO₄ electrolyte, over the electric potential range from 0 to 1 V using voltage scan rate of 100mV/s. The non-linear growth of I-V curves under any of PS or GS conditions, resulting from the nearly rectangle curves without redox peaks that were obtained in the tested potential range, indicating the existing of a high capacitive behavior with a good response of ion (or charge carrier) transfer. The result show that, as the electric potential (V) reaches one volt the current (I) start to decay to minimum value until the electric potential (V) reaches zero. The growth and decay I-V curves forming a rectangular loop of area representing the stored electric energy per unit time as a result of MnO₂ polarization. The calculated stored electric power within the formed supercapacitor is the best way to select PS or GS deposition method for the energy storage.

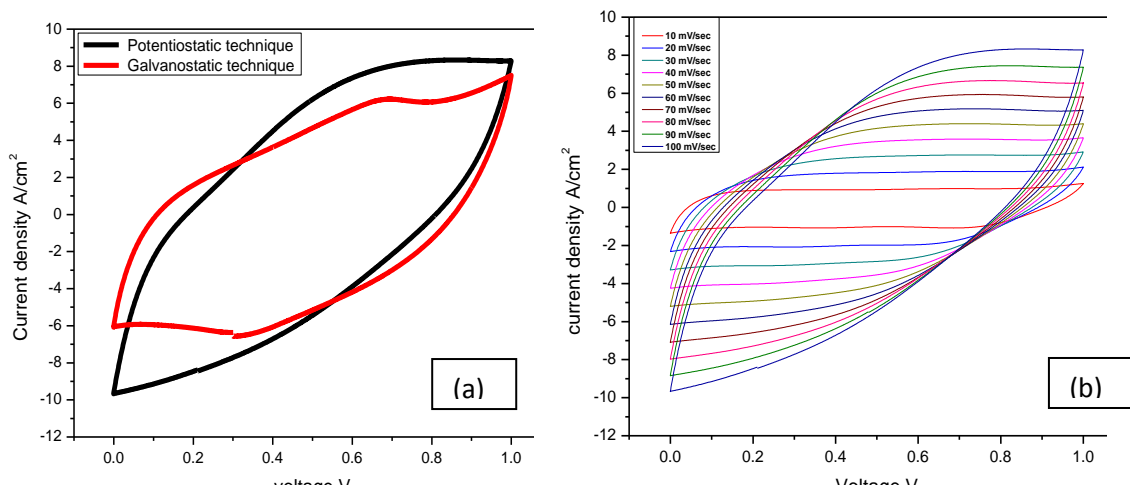


Fig.(3a) I-V curves of (PS) and (GS) deposited MnO₂ films measured in 0.5 M Na₂SO₄ electrolyte at scan rate of 100 mv/s and (b) I-Vcurves of (PS) deposited MnO₂ films at different scan rates.

The values of maximum and average stored power parameters using both PS and GS methods were 18 watt and 6.2 watt, for PS and 12 and 6 watt for GS respectively. These results confirm that PS deposition method is the best to store electric power when used as a supercapacitor. Fig (3b) shows that at a higher rate of scan rate voltage (100 mv/s), the calculated maximum stored electric power was 19 watt, while the average stored electric power was only 6 watt. This means that, the stored electric power is independent on the voltage scan rate. This may attributed to the maximum limit of the electric polarization of MnO₂ i.e. maximum capacity of the constructed supercapacitor. The specific capacitance of the supercapacitor was calculated as a function of the voltage scan rate, for both PS and GS deposition methods Fig (4). This relation varying, the basic capacity potential relation on one hand. On the other hand ensure that, the capacity of deposited layer of MnO₂ using PS method is generally higher and it is the best method to construct supercapacitor of higher capacity.

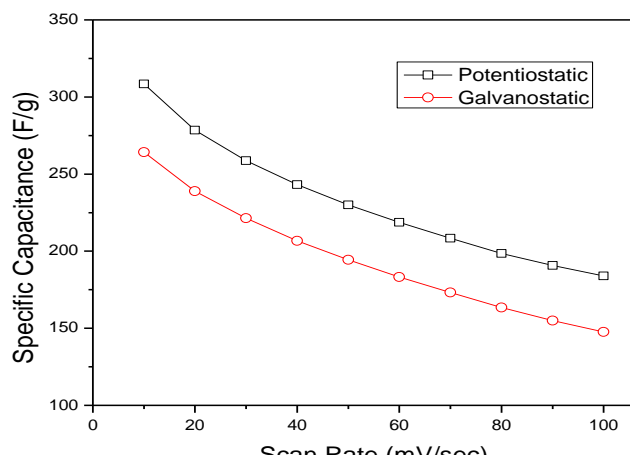


Fig.(4)Dependence of specific capacitance on voltage scan rate for both tested PS and GS deposited MnO₂ films.

The specific capacitance of the constructed supercapacitor was recorded once again as a function of the current density using PS and GS deposition method, fig(5). It is clear that, the specific capacitance decreases as current density increases for both PS and GS. Also at any current density value the value of the specific capacitance from PS was higher than its value from GS. The highest capacity values were 389 and 327 F/g for PS and GS respectively.

This result is in a good agreement with that extracted from the capacity volt relation and confirms it completely.

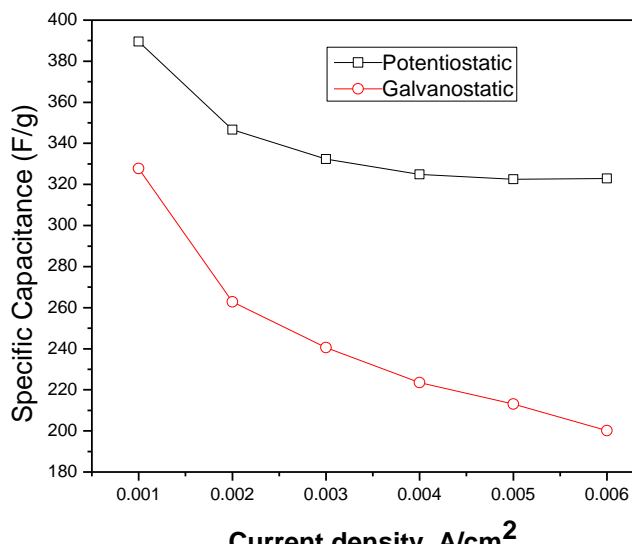


Fig.(5)Dependence of specific capacitance on the current density for both tested PS and GS deposited MnO₂ films

Otherwise, the PS technique is the best one to be constructed, supercapacitor to store electric energy. The stored electric energy on the constructed supercapacitors was calculated and tabulated in table (1).

Voltage scan rate (mv/s)	Energy (Joules) for PS method	Energy (Joules) for GS method
10	1.54 x10 ⁻²	1.32 x10 ⁻²
20	5.56 x10 ⁻²	4.78 x10 ⁻²
30	11.64 x10 ⁻²	9.96 x10 ⁻²
40	19.36 x10 ⁻²	16.48 x10 ⁻²
50	28.75 x10 ⁻²	24.25 x10 ⁻²
60	39.3 x10 ⁻²	32.8 x10 ⁻²
70	51.00 x10 ⁻²	42.1 x10 ⁻²
80	63.36 x10 ⁻²	47.84 x10 ⁻²
90	76.95 x10 ⁻²	62.38 x10 ⁻²
100	91.00 x10 ⁻²	73 x10 ⁻²

According to table (1), it is clear that, the stored energy increases as voltage scan rate increases even using either PS or GS deposition methods. Also, the stored energy using PS method is three by two times, the stored energy using GS method. This may confirm that the MnO₂ polarization under PS condition is much higher than its value under GS condition.

3.3.2. Charge- discharge characteristics

The charge/discharge processes for the constructed supercapacitor were conducted using PS and GS deposited methods under the condition of 0.5 M Na₂SO₄ electrolyte using different current densities. This cycle was recorded in fig (5) for PS and GS at current density 1 mA/cm².

The charging period was controlled by the well-known relation $I = I_0 e^{-t/\tau}$ where (I) is the current at a given time (t), I₀ is the start current $I_0 = \frac{\epsilon}{R}$ where ϵ is the electromotive force of the given battery and R is the shunt resistance, through which the capacitor start to charge, and τ is the capacitor time constant RC. The charging time period of the capacitor t was 140 seconds using PS method, and 105 seconds using GS method. The time constant of the charging period was 6.02x10⁻³ sec for PS and 5x10⁻³ sec for GS. As a result the shunt resistance for PS was 2x10⁻⁵ Ω and 1.06.10⁻⁵Ω for GS.

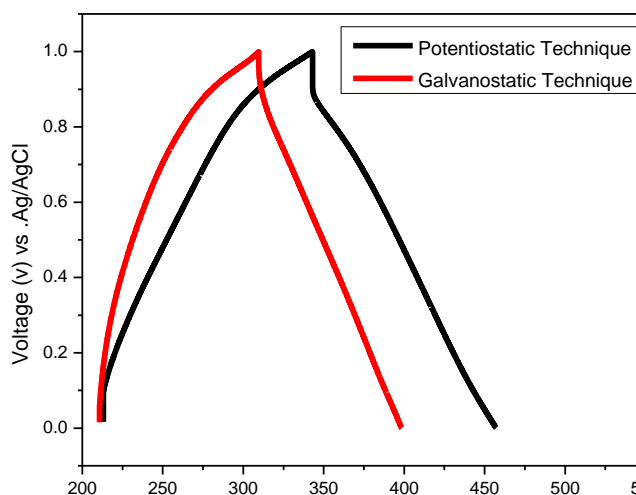


Fig (6) Charge -discharge Voltage-Time curves of both tested PS and GS deposited MnO₂ films at a current density of 1 mA/cm² measured in 0.5 M Na₂SO₄ electrolyte.

Also, the maximum stored potential for PS was 2×10^{-8} volt, while it is for GS 1×10^{-8} volt. Then the main conclusion is that, the potentiostatic (PS) deposition method is the best to store electric energy using supercapacitor technique. During the discharge period, the time constant, RC, for both PS and GS was the same value. Also the shunt resistance was $1.06 \times 10^{-5} \Omega$. These results lead to the electric potential was 1×10^{-8} volt.

3.3.3. Electrochemical impedance spectroscopy (EIS)

Electrochemical impedance spectroscopy measurements were recorded as Nyquist plots for both (PS) and (GS) deposited MnO₂ films on etched SS substrates in 0.5 M Na₂SO₄ electrolyte solution, as shown in Fig.7. It is observed in each plot that an initial high frequency intercept on the real impedance axis at the beginning of the semi-circle corresponding to the equivalent series resistance (ESR), which includes the ionic resistance of the electrolyte, resistance of the active material, resistance of the current collector, and the contact resistance at electrode/electrolyte interface.

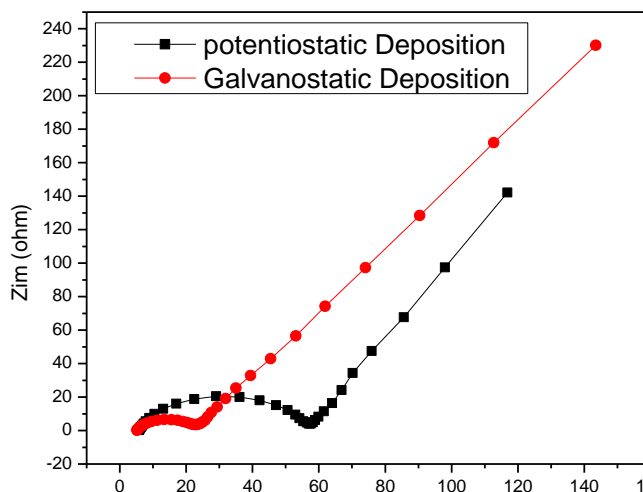


Fig.(7) Nyquist plots of both PS and GS MnO₂ deposited films investigated in 0.5 M Na₂SO₄ electrolyte in the frequency range of 10 MHz –100 kHz at 10 mV amplitude.

In the high frequency region, there is a small semicircle that represents the dominant resistance behavior of the supercapacitor and corresponds to the charge transfer resistance (R_{ct})^{2, 21}. i.e. interfacial reaction kinetics. The electrode possibly blocks the ion exchange of faradic process at the electrode/electrolyte interface. The value of R_{ct} can be derived from the diameter of the semicircle^{2, 22}.

Finally, a linear region at low frequency range is obtained due to Warburg diffusion impedance, the beginning of the linear part represents the combination of resistive and capacitive behaviours of the ions

penetrating into the electrode pores. As the frequency decreases, the capacitive behaviour dominates which results from the formation of the electric double layer system at the electrolyte/electrode interface; in this region, the ions can more easily diffuse into the micro-pores. This means that, the impedance plots show typical features of porous electrode, i.e. resistance at high frequency and capacitance at low frequency^{23, 24}.

Referring to Fig.(5), and fitting of Nyquist plots, the estimated ESR values for both PS and GS deposited films are 5.72Ω and 5.15 Ω, respectively. The slight decrease in the ESR of the GS deposited film might reflect the higher charge carrier density of GS deposited MnO₂ film due to the heterogenous arrangement of that film on the SS substrate. On the other hand, the estimated R_{ct} values for both PS and GS deposited MnO₂ films are 52.88Ω and 19.29 Ω, respectively. The apparent decrease in the charge transfer value of the GS deposited MnO₂ film indicates the enhancement in the electronic and ionic conductivities of the amorphous regions in that film. The short Warburg line for PS deposited MnO₂ film reflects rapid ion diffusion in its porous structure and hence higher specific capacitance. This fact is in a good agreement with the SC data.

3.4. Cyclic Stability:

The electrochemical stability (life cycle) of the tested (PS) and (GS) deposited MnO₂ films are investigated by repeating the charging–discharging process 1000 times at current density 2mA/cm² for each of them, and the results obtained are illustrated in Fig.8.

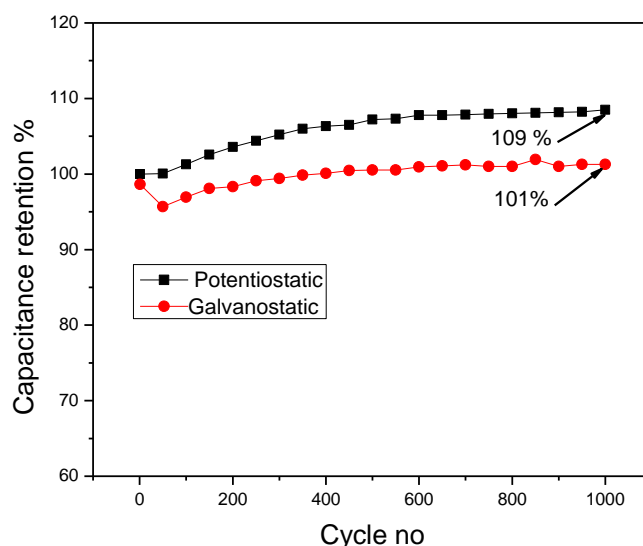


Fig.(8) Life-cycle data of PS and GS deposited MnO₂ films at current density 2 mA/cm²

Figure(8) shows the dependence of capacitance retention on the cycle number of charge-discharge process of both PS and GS films, respectively. As seen, a little increase in the specific capacitance is observed in the case of potentiostatic deposited only MnO₂ film i.e. 0.09% of its initial value after 1000 cycles. However, this is an indication of excellent long term electrochemical cycling stability without fluctuations in the tested potentiostatic deposited MnO₂ films.

IV. CONCLUSION

MnO₂ films were anodically electrodeposited on etched stainless steel current collector from manganese acetate solution by applying two techniques potentiostatic(PS) and galvanostatic(GS). The morphology of (PS) film shows small spherical grains in nano-scale, but (GS) film revealed rough surface. According to electrochemical measurements (PS) electrode exhibited the high specific capacitance of 389F/g at current density 1mA/cm². The specific capacitance of the (PS) electrode has excellent stability during 1000 cycles at a current density of 2mA/cm². The excellent capacitive behavior shows that the amorphous potentiostatically deposited MnO₂ film on 304-stainless steel current collectors can be considered as a promising electrode material for high performance supercapacitors.

ACKNOWLEDGEMENTS

This work was financially supported by Science & Technology Development Fund(STDF), Egypt, Grant No 13855, and Scientists for Next Generation (SNG) Grant, Academy of Scientific Research and Technology in Egypt.

REFERENCES

- [1] A. González, E. Goikolea, J. A. Barrena and R. Mysyk, *Renewable and Sustainable Energy Reviews* 58, 1189-1206 (2016).
- [2] S. Hassan, M. Suzuki and A. Abd El-Moneim, *MATERIALS American Journal of Materials Science* 2 (2), 11-14 (2012).
- [3] D.-D. Zhao, Z. Yang, E. S.-W. Kong, C.-L. Xu and Y.-F. Zhang, *Journal of Solid State Electrochemistry* 15 (6), 1235-1242 (2011).
- [4] Suhasini, *Journal of Electroanalytical Chemistry* 690, 13-18 (2013).
- [5] T. Meynard, A. Schneuwly and R. Gally, *PROCEEDINGS OF THE INTERNATIONAL INTELLIGENT MOTION CONFERENCE* (37), 85-186 (2000).
- [6] Y. Zhao, Y. Y. Wang, Q. Y. Lai, L. M. Chen, Y. J. Hao and X. Y. Ji, *Synthetic Metals* 159 (3-4), 331-337 (2009).
- [7] T. Shinomiya, V. Gupta and N. Miura, *Electrochimica Acta* 51 (21), 4412-4419 (2006).
- [8] P. Sharma and T. S. Bhatti, *Energy Conversion and Management* 51 (12), 2901-2912 (2010).
- [9] Y. R. Ahn, M. Y. Song, S. M. Jo, C. R. Park and D. Y. Kim, *Nanotechnology*. 17 (12), 2865-2869 (2006).
- [10] V. D. Patake, C. D. Lokhande and O. S. Joo, *Applied Surface Science* 255 (7), 4192-4196 (2009).
- [11] C.-C. Hu, Y.-H. Huang and K.-H. Chang, *Journal of Power Sources* 108 (1-2), 117-127 (2002).
- [12] J. Yan, T. Wei, J. Cheng, Z. Fan and M. Zhang, *Materials Research Bulletin* 45 (2), 210-215 (2010).
- [13] J. Jiang and A. Kucernak, *Electrochimica Acta* 47 (15), 2381-2386 (2002).(2011).
- [14] K. y. Liu, Y. Zhang, W. Zhang, H. Zheng and G. Su, *TRANSACTIONS- NONFERROUS METALS SOCIETY OF CHINA -ENGLISH EDITION-* 17, 649-653 (2007).
- [15] M. Winter and R. J. Brodd, *Chemical Reviews* 104 (10), 4245-4270 (2004).
- [16] X.-M. Liu, S.-Y. Fu and C.-J. Huang, *Powder Technology* 154 (2-3), 120-124 (2005).
- [17] G. M. Jacob and I. Zhitomirsky, *Applied Surface Science* 254 (20), 6671-6676 (2008).
- [18] G. A. M. Ali, M. M. Yusoff, Y. H. Ng, H. N. Lim and K. F. Chong, *Current Applied Physics* 15 (10), 1143-1147 (2015).
- [19] D. P. Dubal, D. S. Dhawale, T. P. Gujar and C. D. Lokhande, *Applied Surface Science* 257 (8), 3378-3382 (2011).
- [20] B. E. Conway, *Electrochemical supercapacitors : scientific fundamentals and technological applications*. (Kluwer Academic, Plenum Publishers, New York [u.a.], 1999).
- [21] A. Izadi-Najafabadi, D. T. H. Tan and J. D. Madden, *Synthetic Metals* 152 (1), 129-132 (2005).
- [22] A. Gouda, N. K. Allam and M. A. Swillam, *RSC Advances* 7 (43), 26974-26982 (2017).
- [23] A. Bello, F. Barzegar, M. J. Madito, D. Y. Momodu, A. A. Khaleed, T. M. Masikhwa, J. K. Dangbegnon and N. Manyala, *Electrochimica Acta* 213, 107-114 (2016).

M.M.El-Zaidia. "Energy Storage Using MnO₂ Supercapacitor Electrode." *IOSR Journal of Engineering (IOSRJEN)*, vol. 7, no. 9, 2017, pp. 14-21.